Real-time X-ray scattering studies on temperature dependence of perfluoropentacene thin film growth

C. Frank,[1] J. Novák,[1] A. Gerlach,[1] G. Ligorio,[1] K. Broch,[1] A. Hinderhofer,[1] A. Aufderheide,[1] R. Banerjee,[1] R. Nervo,[2] and F. Schreiber[1]
[1]*Institut für Angewandte Physik, Universität Tübingen, Auf der Morgenstelle 10, 72076 Tübingen, Germany*
[2]*ESRF, 6 Rue Jules Horowitz, BP 220, 38043 Grenoble Cedex 9, France*

(Received 19 April 2013; accepted 8 July 2013; published online 25 July 2013)

We report on real-time scattering investigations of growth of thin films of Perfluoropentacene (PFP) and its dependence on the substrate temperature, ranging between −120 °C and 60 °C. All films were grown up to 50 nm on silicon oxide. We find that along with the known thin-film phase, there is also a coexisting molecular arrangement with a unit cell twice the size with respect to the long axis. Furthermore, we observe that even at temperatures as low as −20 °C PFP shows a high degree of crystallinity in the out-of-plane direction. The growth of PFP is characterized by a two-stage process, where the molecular lattice experiences a much stronger in-plane relaxation in the thickness regime 0–19 nm compared to the thickness regime 19–50 nm, which can be probed only by *in situ* real-time scattering measurements. © *2013 AIP Publishing LLC*.
[http://dx.doi.org/10.1063/1.4816320]

I. INTRODUCTION

In recent years, significant effort has been made to investigate structural and optical properties of organic materials with potential for device applications.[1,2] In this context, perfluoropentacene (PFP, $C_{22}F_{14}$) is a promising n-type organic semiconductor.[3–7] Relative to its hydrogenated counterpart pentacene (PEN, $C_{22}H_{14}$),[8] PFP may serve as an electron acceptor.[9,10] In particular, shifting the HOMO/LUMO energy levels via fluorination may provide an efficient way to tailor electronic properties, such as the electron injection barrier.[11–17] In the developing field of organic electronics, this offers interesting possibilities to combine such p- and n-type semiconductors either in heteroplanar[18,19] or mixed[20,21] structural configurations. However, while PEN has been thoroughly studied,[9,22,23] reports on the structure of PFP are still scarce.[24–33]

The investigation of structure and morphology of PFP is of prime importance, since the electronic and steric compatibility with PEN offers interesting perspectives. Real-time X-ray studies have been proven to be an extremely powerful, non-invasive technique to study the growth of inorganic and organic materials,[34] in particular when utilizing new detector technologies combined with high brilliance synchrotron radiation. For devices based on thin films, the degree of crystallinity significantly influences the charge carrier mobility of organic semiconductors.[35] To optimize this for possible device aplications, it is important to be able to tune the crystallinity of PFP, which is strongly connected to diffusion processes during growth, by changing the substrate temperature. In this work, we investigate the effect of the substrate temperature on the structure of PFP films prepared by organic molecular beam deposition (OMBD). Generally, OMBD is a non-equilibrium and dynamic process. Molecules may reorganize even after impinging on the sample surface and transient structures may arise.[36–38] This dynamic nature already implies the need for time-resolved studies to obtain a full understanding of how different growth parameters influence the thin-film properties, structurally as well as optically or electronically.[27–29,39,40]

One of the crucial parameters controlling the growth dynamics, which may also lead to polymorphism, is the substrate temperature.[41–45] The scope of this work is to follow the structural evolution of PFP thin films at different substrate temperatures, by using X-ray scattering techniques in a wide angle regime and in real-time (i.e., with a sub-monolayer resolution) during growth. The results are complemented by atomic force microscopy (AFM) studies.

We observe a so far unreported coexistence of a phase with a molecular arrangement in a unit cell twice the size with respect to the long axis together with the known thin-film phase. We also observe that PFP is highly crystalline and grows as a 2D-powder even at a growth temperature as low as −20 °C. Employing *in situ* real-time scattering measurements we establish that the growth of PFP is characterized by a two-step process. In thickness regime I (0–19 nm) the molecular lattice experiences a much stronger in-plane relaxation compared to regime II (19–50 nm).

II. EXPERIMENTAL

The substrates were cleaned using an ultrasonic bath with acetone, iso-propanol, and ultra-pure water. Purified PFP ($\geq 99\,\%$) was purchased from Kanto Denka Kogyo Co. and deposited on commercial silicon wafers with a native oxide layer (SiO_x). PFP films were grown via OMBD in a portable UHV-chamber (base pressure $<8 \times 10^{-9}$ millibars).[46] The growth rate was approximately 3 Å/min and verified by a water-cooled quartz crystal micro-balance. The substrate temperature was changed in a wide range from −120 °C to 60 °C. A beryllium window allows entry and exit of X-rays, which facilitates following the growth in real time. Using synchrotron radiation, reciprocal space maps (RSMs) in the grazing incidence diffraction (GID) regime and post-growth

scans were measured either with a point detector or with a Pilatus-II detector, *in situ* at the ID10B end station ($\lambda = 1.0754$ Å) at the European Synchrotron Radiation Facility in Grenoble. *Ex situ* samples were characterized in our in-house laboratory via AFM, X-ray reflectivity (XRR) and rocking-scans. AFM images were measured in tapping mode with a JPK Nanowizard II instrument and post processed with the free software package Gwyddion.[47] XRR and rocking-scans were measured with a GE XRD3003 diffractometer ($CuK_{\alpha 1}$).

III. RESULTS AND DISCUSSION

In post-growth AFM studies, we observed that changing the substrate temperature results in very different film morphologies, see Fig. 1 showing AFM images of 50 nm PFP grown at 60 °C and −20 °C, respectively. At a substrate temperature of 60 °C PFP forms long needle-like crystallites several micrometers in length. The Root Mean Square (RMS)-roughness is ∼7 nm, i.e., relatively smooth compared to the final nominal film thickness of 50 nm. The corresponding height-distribution of the crystallites is shown in the inset of Fig. 1(a). The distribution has a sharp maximum at a height of $z \approx 28$ nm and has a Full Width at Half Maximum (FWHM) of $\Delta_z \approx 15$ nm. Similar morphologies have been reported in previous studies,[22,27,48] where PFP was grown either at high temperatures or close to room temperature. In contrast, for the growth at −20 °C (Fig. 1(b)) the thin film is formed by small mounds with heights up to 500 nm and diameters up to 500 nm. (Note that a smaller scan area is shown, which does not display artifacts caused by the film morphology.) The film is very jagged and a precise quantification of the film surface parameters is beyond the capabilities of the employed AFM. Hence, the AFM images already suggest a better ordering of PFP molecules in films grown at high temperatures.

The out-of-plane film structure can be characterized by XRR. Figure 2(a) shows XRR-scans of two 50 nm PFP *ex situ* samples, which were grown at substrate temperatures

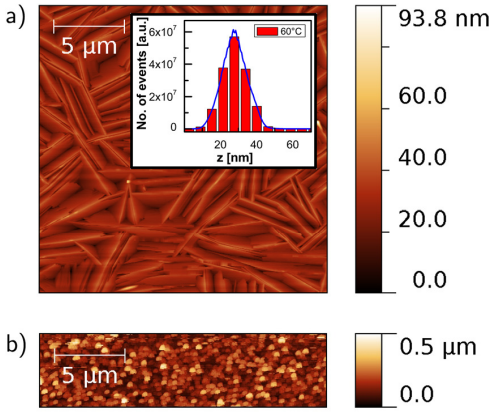

FIG. 1. AFM images of 50 nm PFP grown at a substrate temperature of (a) 60 °C and (b) −20 °C. The images cover a scan area of $20 \times 20\ \mu m^2$ and $20 \times 5\ \mu m^2$, respectively. The inset shows the corresponding height-distributions at 60 °C.

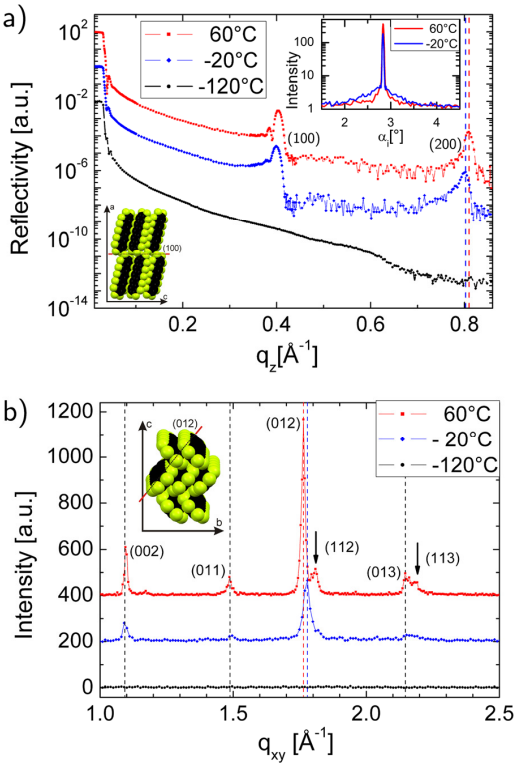

FIG. 2. (a) XRR-scans of PFP grown at 60 °C (red), −20 °C (blue), and −120 °C (black). Additionally, rocking scans were performed on the (100)-Bragg reflections. (b) GID-scans of PFP grown at 60 °C (red), −20 °C (blue), and −120 °C (black). XRR- and GID-scans are vertically shifted for clarity in (a) and (b). The molecular packing of PFP is shown as an inset in perpendicular (a) and parallel (b) direction to the sample surface. (100) and (012) scattering planes are indicated with dashed lines.

of 60 °C (red) and −20 °C (blue), respectively. For both temperatures, Bragg reflections $(h00)$ up to the 2nd order can be observed. The indexing throughout the manuscript is chosen in compliance with Ref. 23, which means that the long molecular axis is assigned to axis a (see bottom left inset of Fig. 2(a)). Note that at a substrate temperature of −120 °C no Bragg reflections are found. For 60 °C well pronounced Kiessig- and Laue oscillations are observed. From the respective periodicities the total and the coherent film thickness are estimated to be $D_{tot} = 566 \pm 36$ Å and $D_{coh} = 402 \pm 18$ Å. The out-of-plane lattice spacing is derived from the second Bragg peak including a refractive correction for the PFP-layer. The lattice parameter $a = 15.52 \pm 0.02$ Å, agrees well with that of the PFP single crystal phase, reported by Sakamoto *et al.*[23] For growth temperatures of −20 °C Kiessig- and Laue-oscillations are rapidly damped due to the higher roughness of the film. The out-of-plane lattice parameter is $a = 15.70 \pm 0.02$ Å, i.e., we observe a change in the lattice parameter by $\Delta a \approx 0.2$ Å compared to 60 °C. This increase of the lattice parameter upon decreasing the substrate temperature obviously implies a slight rearrangement of the molecular packing.

The in-plane film structure is explored by GID-scans performed post-growth with a point detector for low and

high temperatures. For −20 °C and 60 °C (see Fig. 2(b)), the observed in-plane Bragg-reflections are close to the reported thin-film structure.[27] The absence of in-plane Bragg reflections for −120 °C is consistent with amorphous film growth of PFP at very low temperatures. Comparing the in-plane peak positions in Fig. 2(b) for 60 °C and −20 °C (see dashed lines) we observe a peak-shift in the 012-direction. Decreasing the temperature obviously leads to a shift of $\Delta(012) = 0.016\,\text{Å}^{-1}$, which corresponds to a lattice expansion of $\Delta_d = 0.032$ Å in the 012-direction. Close to the (012) and (013) Bragg reflections two peaks (marked by arrows) are observed for 60 °C. We attribute these peaks to the projection of the (112)- and (113)-Bragg reflections onto the q_{xy} plane.

A better understanding of growth mechanisms can be obtained by taking advantage of the most recent detector technology with high dynamic range, high signal-to-noise ratio and faster acquisition and read-out times, which provides unprecedented spatial and temporal resolution. *In situ* RSMs were taken during growth and post-growth in the GID-regime. Post-growth RSM images are shown in Figs. 3(a) and 3(b) for the substrate temperatures 60 °C and −20 °C. Note that at −120 °C (image not shown here) no diffraction peaks are visible, similar to the XRR/GID-scans. At 60 °C well-defined crystal truncation rods (CTRs) are observed for all diffraction orders *hkl*. In contrast, CTRs are broader and more diffuse at −20 °C. This suggests that at low temperatures the projection of the coherent scattering volume onto the sample surface is smaller. Furthermore, the absence of diffraction rings for both temperatures indicates that PFP-molecules grow in a 2D-powder structure on SiO_x-substrates. This is confirmed by rocking-scans, which are taken on the first Bragg reflection (see top right inset in Fig. 2(a)). At both temperatures a similar mosaicity is observed but with a higher diffuse background at low temperatures. PFP exhibits a high degree of crystallinity perpendicular to the sample surface when it is grown on SiO_x at elevated substrate temperatures. This is evident from our measurements here and also corroborates earlier studies.[27] However, the fact that the structure is also crystalline even at a temperature as low as −20 °C was not reported earlier and is established in this study.

At 60 °C, surprisingly, a series of weak $(\frac{1}{2}kl)$ diffraction peaks is observed (Fig. 3(a)). Evaluating their positions along the q_z-rods (see Fig. 3(c) for the $(h12)$- and $(h02)$-rod), results in $q_z = 0.211\,\text{Å}^{-1}$, i.e., half the q_z-value of the first order Bragg reflections. Therefore, we conclude that a coexisting phase with a unit cell two times larger along the *a* axis than the dominating PFP thin-film phase[22,27] (with two molecules per unit cell) nucleates. This indicates that two molecules are arranged along the *a* axis of the unit cell, as was also observed, e.g., for poly(p-phenyl)oligomers.[49] In contrast, at −20 °C the $(\frac{1}{2}kl)$ diffraction peaks are weaker (see also Fig. 3(c)). We speculate that the phase with the long axis doubled is on the one hand energetically more favored and its nucleation is on the other hand thermally activated. Thus, it is not present at low temperatures. In addition, at both substrate temperatures we observe a CTR next to the $(h13)$-rod, which to our knowledge has not been reported yet. Note that line scans of the $(h11)$ and $(h13)$ CTR's are shown in Ref. 50.

The evolution of the in-plane grain size is of significant interest, because in previous studies it was observed that the ordering behavior of organic materials can be very different in the in-plane and the out-of-plane direction.[51] For the real-time data analysis, we have taken series of RSM-images *in situ* at −20 °C and 60 °C during the film growth with sufficient time resolution, i.e., the time between two images corresponds to ∼0.5 ML (mono-layer). Focusing on the in-plane information we restrict ourself to the (012)-diffraction peak, which is the strongest in-plane reflection with the best signal-to-noise ratio. Using the stronger (112)-reflection would also be possible, but in this case we would have a considerably large q_z-component, thus yielding a superposition of in-plane and out-of-plane information. For the following analysis, intensities are integrated within a region-of-interest (ROI), which is defined around the (012)-Bragg reflection (indicated by blue rectangles in Fig. 3).

Figure 4(a) shows the integral intensity plotted as a function of the nominal film thickness. At 60 °C the intensity increases linearly, which indicates the virtually ideal polycrystallinity of PFP grown at high substrate temperatures. In contrast, at −20 °C the intensity increases in a non-linear fashion and starts to saturate at the film thickness of ∼20 nm. Obviously, there are more crystal defects at low temperatures leading to a decrease of the coherent scattering crystal size parallel to the substrate plane. Additionally, at −20 °C there may well exist an amorphous fraction of material, which does not contribute to the coherent scattering, therefore, resulting in a film thickness dependent loss of scattering intensity.

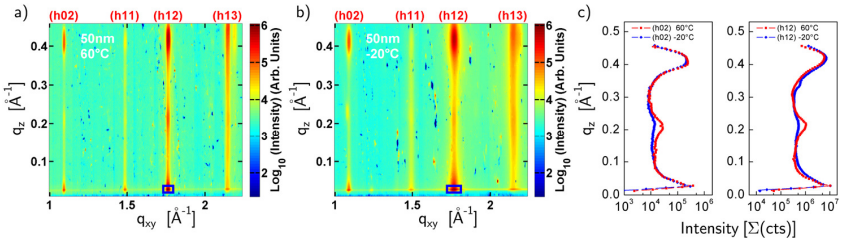

FIG. 3. (a) RSM of 50 nm PFP grown at a substrate temperature of 60 °C. (b) RSM of 50 nm PFP grown at a substrate temperature of −20 °C. Blue rectangles mark the (012)-Bragg reflection, which is used for the real-time data analysis. (c) Diffuse intensity in the vicinity of the $(h02)$ and $(h12)$ CTRs. The intensities are extracted from the post-growth RSMs and are integrated along q_{xy}-direction. At 60 °C a diffraction peak is observed most evidently at $(\frac{1}{2}12)$, which nearly disappears at −20 °C. Note that the intensities of the 60 °C and −20 °C line-scans as well as the RSMs were normalized to a common maximum.

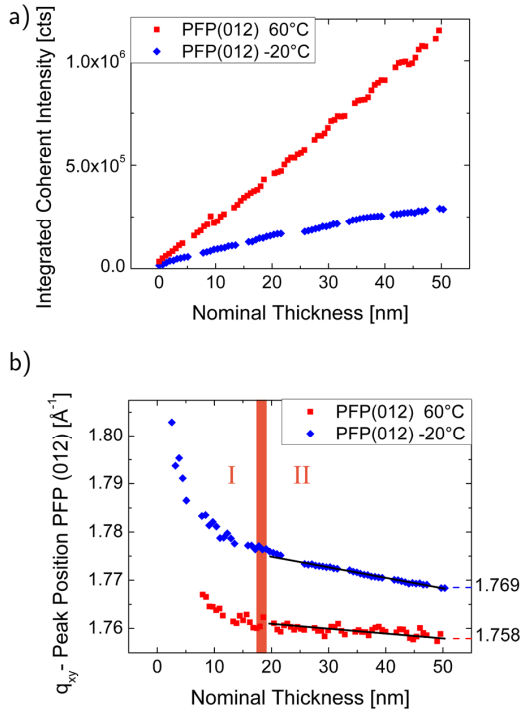

FIG. 4. (a) Integrated intensity of the (012)-Bragg reflection, plotted against the nominal film thickness for 60 °C (red) and −20 °C (blue). (b) Position of the (012) diffraction peak plotted against the nominal film thickness for 60 °C (red) and −20 °C (blue). Fitting of the peak position was not possible at the initial stage of growth as the signal-to-noise ratio was too low. Black lines indicate the tentative trend of the temporal evolution in regime II.

To gain real-time information on grain size and lattice spacing we integrate intensities within the ROI along the q_z-direction to obtain a line scan with intensity as a function of q_{xy}. For both temperatures such line-scans were fitted with a double pseudo-Voigt profile, which was applied, to take the influence of the (112)-diffraction peak at 60 °C into account. From the fits the position of the peak as well as the FWHM were obtained. The evolution of the peak position as a function of nominal film thickness is shown in Fig. 4(b). At both temperatures two regimes can be distinguished. The early stage of the growth, labeled as regime I, corresponds to a nominal film thickness of $d \approx 0$–19 nm (i.e., $d \approx 0$–12 ML). At this stage, the (012)-diffraction peak shifts rapidly in a non-linear fashion towards smaller q_{xy}, which means that for thin films of PFP, i.e., up to $d \approx 12$ ML, a significant relaxation of the lattice occurs. Regime II characterizes thicker films of PFP ($d \approx 19$–50 nm). At both temperatures the change of the lattice parameter is now linear and (as indicated by black lines in Fig. 4(b)) much slower. Additionally, it is observed that at 60 °C the peak shift is smaller than at −20 °C. This signifies that for PFP grown at 60 °C a relevant relaxation of the lattice takes place only until a critical film thickness of approximately 12 ML, in contrast to a substrate temperature of −20 °C. For thicker high temperature PFP films no significant modification of the lattice is expected. The final difference of the lattice parameter in 012-direction between both highlighted temperatures is $\Delta q_{xy} = 0.011$ Å^{-1}, which corresponds to a real space expansion of $\Delta d = 0.022$ Å. Within the experimental resolution this agrees well with the temperature related shift of the (012)-Bragg reflection observed in the post-growth GID-scans (see Fig. 2(b)). The evolution of the coherent island size d_s in the in-plane direction (see Fig. 5) is obtained via the Scherrer-formula, i.e., $2\pi/\Delta q_{xy}$, where Δq_{xy} was corrected for the resolution function

$$\Delta q_{xy} = \sqrt{\Delta q_{CCD}^2 - \Delta q_{res}^2}.$$

Here, Δq_{CCD}^2 is the FWHM, which is obtained by fitting the (012)-peak in the RSMs and Δq_{res}^2 is the FWHM of the resolution function. At −20 °C the in-plane coherent island size evolves very fast during the deposition of the first 5 nm. Subsequently, the island size increases linearly until a final size of $d_s = 24$ nm is reached. Since the experimental resolution limits the determination of the in-plane-island size to $d_s \approx 25$ nm, we were not able to follow the evolution at the high substrate temperature. However, by analyzing the 60 °C post-growth GID-scan the final island size is determined to be $d_s \approx 44$ nm. Therefore, we conclude that for high temperature PFP growth, islands evolve in-plane in 012-direction rapidly, i.e., within a few ML, to a size beyond 25 nm.

Combining these results, we suggest a temperature dependent structure of PFP thin films as proposed in Fig. 6. At low temperatures the surface diffusion of molecules is limited. This leads to the formation of dislocations in the lattice resulting in smaller crystallites. As the film grows the lattice experiences a strong relaxation, i.e., structural re-arrangement of molecules until a critical thickness of approximately 12 ML is reached. Subsequent ML rearranges in a much more facile way. Crystallites are defined by grain boundaries, which, on the one hand decrease the coherent scattering volume, and on the other hand increase the contribution of diffuse scattering. Therefore, the final film is composed of relatively small crystallites exhibiting a low crystalline order in the in-plane direction. At elevated substrate temperatures the diffusion is stronger. Therefore, less dislocations are incorporated in the lattice resulting in larger crystallites. The crystallinity is significantly enhanced in the in-plane

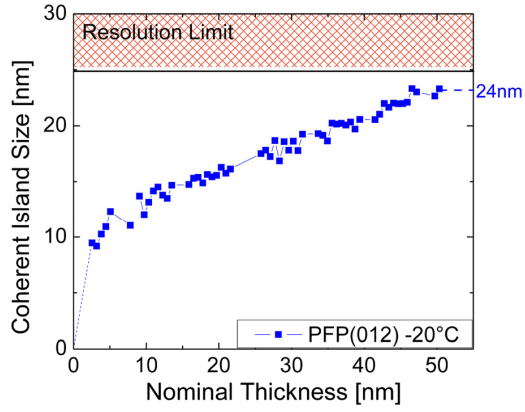

FIG. 5. Evolution of the in-plane coherent island size in 012-direction as a function of nominal film thickness for −20 °C.

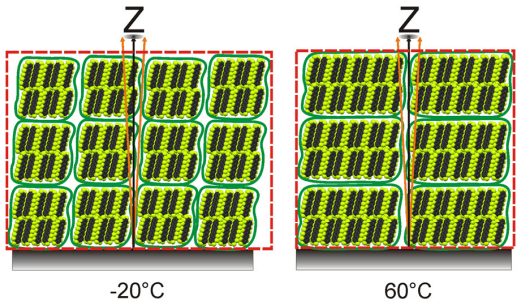

FIG. 6. Suggested growth of PFP-crystallites at −20 °C (left) and 60 °C (right). The scattering volume is indicated by a dashed red line. Due to smaller crystallite sizes at −20 °C we expect a larger amount of domain boundaries (green lines) lying within the coherently scattering volume. The possible occurrence of an amorphous fraction of material is not shown in the sketch.

direction, i.e., better long-range order compared to low temperatures. The relaxation of the lattice is much weaker and beyond a critical thickness molecules barely re-arrange.

IV. SUMMARY AND CONCLUSION

This study gives an account of the temperature dependent structure and morphology of PFP thin films with thicknesses up to 50 nm prepared by OMBD on SiO_x-substrates. At growth temperatures of 60 °C lying needle-like crystallites, several microns in length, are formed composed of smaller grains with an average size of 44 nm. Interestingly and so far unreported, a crystal phase containing four molecules per unit cell is observed. In contrast, at growth temperatures of −20 °C thin films are composed of mounds of diameter and height ~500 nm. The final grain size is reduced to 22 nm. At growth temperatures of −120 °C we observe a fully amorphous film growth. A compression of the lattice parameters in the in-plane direction ($\Delta d/d(012) = 0.91\%$) and their dilatation in the out-of-plane direction ($\Delta a/a(h00) = 1.29\%$) is observed between growth temperatures of −20 °C and 60 °C.

Real-time *in situ* studies provide evidence for different kinetics of grain formation for low and high temperatures. In particular, we suggest a growth model where the crystallinity in the in-plane direction is affected by the substrate temperature, whereas in the out-of-plane direction it does not depend significantly on the temperature.

Since the crystalline order is strongly connected to electronic transport properties, tuning the substrate temperature together with the film thickness may therefore be considered as a promising method to tailor the structure in device applications.

ACKNOWLEDGMENTS

We gratefully acknowledge financial support by the DFG (Deutsche Forschungsgemeinschaft).

[1]F. Yang, M. Shtein, and S. R. Forrest, Nature Mater. **4**, 37 (2005).
[2]A. Hinderhofer and F. Schreiber, ChemPhysChem **13**, 628 (2012).
[3]J. E. Anthony, A. Facchetti, M. Heeney, S. R. Marder, and X. Zhan, Adv. Mater. **22**, 3876 (2010).
[4]T. Breuer, M. A. Celik, P. Jakob, R. Tonner, and G. Witte, J. Phys. Chem. C **116**, 14491 (2012).
[5]L. Huang, D. Rocca, S. Baroni, K. E. Gubbins, and M. B. Nardelli, J. Chem. Phys. **130**, 194701 (2009).
[6]N. G. Martinelli, Y. Olivier, S. Athanasopoulos, M.-C. R. Delgado, K. R. Pigg, D. A. da Silva Filho, R. S. Sánchez-Carrera, E. Venuti, R. G. D. Valle, J.-L. Brédas, D. Beljonne, and J. Cornil, ChemPhysChem **10**, 2265 (2009).
[7]I. Salzmann, S. Duhm, G. Heimel, M. Oehzelt, R. Kniprath, R. L. Johnson, J. P. Rabe, and N. Koch, J. Am. Chem. Soc. **130**, 12870 (2008).
[8]J.-Z. Wang, J. T. Sadowski, Z.-H. Xiong, Y. Fujikawa, Q. K. Xue, and T. Sakurai, Nanotechnology **20**, 095704 (2009).
[9]F. Anger, J. O. Ossó, U. Heinemeyer, K. Broch, R. Scholz, A. Gerlach, and F. Schreiber, J. Chem. Phys. **136**, 054701 (2012).
[10]K. Broch, U. Heinemeyer, A. Hinderhofer, F. Anger, R. Scholz, A. Gerlach, and F. Schreiber, Phys. Rev. B **83**, 245307 (2011).
[11]F. Babudri, G. M. Farinola, F. Naso, and R. Ragni, Chem. Commun. **2007**, 1003.
[12]S. Duhm, I. Salzmann, G. Heimel, M. Oehzelt, A. Haase, R. L. Johnson, J. P. Rabe, and N. Koch, Appl. Phys. Lett. **94**, 033304 (2009).
[13]S. Duhm, S. Hosoumi, I. Salzmann, A. Gerlach, M. Oehzelt, B. Wedl, T.-L. Lee, F. Schreiber, N. Koch, N. Ueno, and S. Kera, Phys. Rev. B **81**, 045418 (2010).
[14]N. Koch, A. Vollmer, S. Duhm, Y. Sakamoto, and T. Suzuki, Adv. Mater. **19**, 112 (2007).
[15]B. M. Medina, D. Beljonne, H.-J. Egelhaaf, and J. Gierschner, J. Chem. Phys. **126**, 111101 (2007).
[16]S. L. Wong, H. Huang, Y. L. Huang, Y. Z. Wang, X. Y. Gao, T. Suzuki, W. Chen, and A. T. S. Wee, J. Phys. Chem. C **114**, 9356 (2010).
[17]D. G. de Oteyza, Y. Wakayama, X. Liu, W. Yang, P. L. Cook, F. J. Himpsel, and J. E. Ortega, Chem. Phys. Lett. **490**, 54 (2010).
[18]A. Hinderhofer, A. Gerlach, S. Kowarik, F. Zontone, J. Krug, and F. Schreiber, Europhys. Lett. **91**, 56002 (2010).
[19]A. Hinderhofer, T. Hosokai, C. Frank, J. Novák, A. Gerlach, and F. Schreiber, J. Phys. Chem. C **115**, 16155 (2011).
[20]A. Hinderhofer, C. Frank, T. Hosokai, A. Resta, A. Gerlach, and F. Schreiber, J. Chem. Phys. **134**, 104702 (2011).
[21]J. P. Reinhardt, A. Hinderhofer, K. Broch, U. Heinemeyer, S. Kowarik, A. Vorobiev, A. Gerlach, and F. Schreiber, J. Phys. Chem. C **116**, 10917 (2012).
[22]A. Hinderhofer, U. Heinemeyer, A. Gerlach, S. Kowarik, R. M. J. Jacobs, Y. Sakamoto, T. Suzuki, and F. Schreiber, J. Chem. Phys. **127**, 194705 (2007).
[23]Y. Sakamoto, T. Suzuki, M. Kobayashi, Y. Gao, Y. Fukai, Y. Inoue, F. Sato, and S. Tokito, J. Am. Chem. Soc. **126**, 8138 (2004).
[24]M. C. R. Delgado, K. R. Pigg, D. A. da Silva Filho, N. E. Gruhn, Y. Sakamoto, T. Suzuki, R. M. Osuna, J. Casado, V. Hernández, J. T. L. Navarrete, N. G. Martinelli, J. Cornil, R. S. Sánchez-Carrera, V. Coropceanu, and J.-L. Brédas, J. Am. Chem. Soc. **131**, 1502 (2009).
[25]Y. Inoue, Y. Sakamoto, T. Suzuki, M. Kobayashi, Y. Gao, and S. Tokito, Jpn. J. Appl. Phys. **44**, 3663 (2005).
[26]Y. Sakamoto, T. Suzuki, M. Kobayashi, Y. Gao, Y. Inoue, and S. Tokito, Mol. Cryst. Liq. Cryst. **444**, 225 (2006).
[27]S. Kowarik, A. Gerlach, A. Hinderhofer, S. Milita, F. Borgatti, F. Zontone, T. Suzuki, F. Biscarini, and F. Schreiber, Phys. Status Solidi (RRL) **2**, 120 (2008).
[28]A. R. Woll, T. V. Desai, and J. R. Engstrom, Phys. Rev. B **84**, 075479 (2011).
[29]T. V. Desai, A. R. Woll, F. Schreiber, and J. R. Engstrom, J. Phys. Chem. C **114**, 20120 (2010).
[30]J. Götzen, C. H. Schwalb, C. Schmidt, G. Mette, M. Marks, U. Höfer, and G. Witte, Langmuir **27**, 993 (2011).
[31]K. Fujii, C. Himcinschi, M. Toader, S. Kera, D. R. T. Zahn, and N. Ueno, J. Electron Spectrosc. Relat. Phenom. **174**, 65 (2009).
[32]T. Breuer and G. Witte, Phys. Rev. B **83**, 155428 (2011).
[33]T. Breuer, I. Salzmann, J. Götzen, M. Oehzelt, A. Morherr, N. Koch, and G. Witte, Cryst. Growth Des. **11**, 4996 (2011).
[34]B. Krause, F. Schreiber, H. Dosch, A. Pimpinelli, and O. H. Seeck, Europhys. Lett. **65**, 372 (2004).
[35]A. K. Tripathi and J. Pflaum, Appl. Phys. Lett. **89**, 082103 (2006).
[36]G. Witte and C. Wöll, J. Mater. Res. **19**, 1889 (2004).
[37]F. Schreiber, Phys. Status Solidi A **201**, 1037 (2004).
[38]J. Krug, Physica A **313**, 47 (2002).
[39]U. Heinemeyer, K. Broch, A. Hinderhofer, M. Kytka, R. Scholz, A. Gerlach, and F. Schreiber, Phys. Rev. Lett. **104**, 257401 (2010).

[40]F. Liscio, C. Albonetti, K. Broch, A. Shehu, S. D. Quiroga, L. Ferlauto, C. Frank, S. Kowarik, R. Nervo, A. Gerlach, S. Milita, F. Schreiber, and F. Biscarini, ACS Nano **7**, 1257 (2013).
[41]R. Ruiz, A. C. Mayer, G. G. Malliaras, B. Nickel, G. Scoles, A. Kazimirov, H. Kim, R. L. Headrick, and Z. Islam, Appl. Phys. Lett. **85**, 4926 (2004).
[42]B. Krause, A. C. Dürr, K. Ritley, F. Schreiber, H. Dosch, and D. Smilgies, Phys. Rev. B **66**, 235404 (2002).
[43]P. Fenter, F. Schreiber, L. Zhou, P. Eisenberger, and S. R. Forrest, Phys. Rev. B **56**, 3046 (1997).
[44]L. Kilian, E. Umbach, and M. Sokolowski, Surf. Sci. **573**, 359 (2004).
[45]K. O. Lee and T. T. Gan, Chem. Phys. Lett. **51**, 120 (1977).
[46]K. A. Ritley, B. Krause, F. Schreiber, and H. Dosch, Rev. Sci. Instrum. **72**, 1453 (2001).
[47]D. Nečas and P. Klapetek, Cent. Eur. J. Phys. **10**, 181 (2012).
[48]I. Salzmann, S. Duhm, G. Heimel, J. P. Rabe, N. Koch, M. Oehzelt, Y. Sakamoto, and T. Suzuki, Langmuir **24**, 7294 (2008).
[49]K. N. Baker, A. V. Fratini, T. Resch, H. C. Knachel, W. W. Adams, E. P. Socci, and B. L. Farmer, Polymer **34**, 1571 (1993).
[50]See supplementary material at http://dx.doi.org/10.1063/1.4816320 for the (h11) and (h13) CTRs of PFP films grown at −20 °C and 60 °C.
[51]A. Aufderheide, K. Broch, J. Novák, A. Hinderhofer, R. Nervo, A. Gerlach, R. Banerjee, and F. Schreiber, Phys. Rev. Lett. **109**, 156102 (2012).